

# Bypass Flow Computations Using a One-Twelfth Symmetric Sector for Normal Operation in a 350 MW<sub>th</sub> Prismatic VHTR

HTR 2010

Richard W. Johnson  
Hiroyuki Sato

October 2010

This is a preprint of a paper intended for publication in a journal or proceedings. Since changes may be made before publication, this preprint should not be cited or reproduced without permission of the author. This document was prepared as an account of work sponsored by an agency of the United States Government. Neither the United States Government nor any agency thereof, or any of their employees, makes any warranty, expressed or implied, or assumes any legal liability or responsibility for any third party's use, or the results of such use, of any information, apparatus, product or process disclosed in this report, or represents that its use by such third party would not infringe privately owned rights. The views expressed in this paper are not necessarily those of the United States Government or the sponsoring agency.

The INL is a  
U.S. Department of Energy  
National Laboratory  
operated by  
Battelle Energy Alliance



## Bypass Flow Computations using a One-Twelfth Symmetric Sector for Normal Operation in a 350 MW<sub>th</sub> Prismatic VHTR

Richard W. Johnson and Hiroyuki Sato<sup>1</sup>  
Idaho National Laboratory, Idaho Falls, Idaho, USA  
phone: 208-526-0955, Rich.Johnson@inl.gov

<sup>1</sup>Japan Atomic Energy Agency, Oarai, Ibaraki, Japan

**Abstract** – Significant uncertainty exists about the effects of bypass flow in a prismatic gas-cooled very high temperature reactor (VHTR). Bypass flow is the flow in the gaps between prismatic graphite blocks in the core. The gaps are present because of variations in their construction, imperfect installation and expansion and shrinkage from thermal heating and neutron fluence. Calculations are performed using computational fluid dynamics (CFD) for flow of the helium coolant in the gap and coolant channels along with conjugate heat generation and heat transfer in the fuel compacts and graphite. A commercial CFD code is used for all of the computations. A one-twelfth sector of a standard hexagonal block column is used for the CFD model because of its symmetry. Various scenarios are computed by varying the gap width from zero to 5 mm, varying the total heat generation rate to examine average and peak radial generation rates and variation of the graphite block geometry to account for the effects of shrinkage caused by irradiation. The calculations are for a 350 MW<sub>th</sub> prismatic reactor. It is shown that the effect of increasing gap width, while maintaining the same total mass flow rate, causes increased maximum fuel temperature while providing significant cooling to the near-gap region. The maximum outlet coolant temperature variation is increased by the presence of gap flow and also by an increase in total heat generation with a gap present. The effect of block shrinkage is actually to decrease maximum fuel temperature compared to a similar reference case.

### I. INTRODUCTION

The United States Department of Energy is supporting the development of the next generation nuclear plant (NGNP) as a generation IV passively safe reactor design. The NGNP will be based on one of two possible configurations of very high temperature reactor (VHTR): either the prismatic or pebble bed design. Both reactor concepts are helium cooled. Recently, it was decided to base safety analysis program development for the prismatic concept on the General Atomics modular high temperature gas reactor (MHTGR), which is a 350 MW<sub>th</sub> reactor [1]. The core basically consists of hexagonal graphite blocks that can be viewed as concentric rings of blocks. The first three rings are simply graphite reflector blocks and comprise the inner reflector; the next three rings are fueled blocks with coolant and fuel channels. There are three

additional rings of blocks that form an outer reflector. Figure 1 shows a cross-section of the reactor vessel. There are 66 columns of blocks that contain fuel (seen in a lighter color in the figure.) Figure 2 shows a cross-section of a typical fueled prismatic block, indicating the locations of fuel and coolant channels. Each fueled block is 0.793 m high with distance across the flats of 0.36 m. The core consists of stacks of fueled and reflector blocks. There is an upper reflector that is 1.189 m high, ten fueled blocks below that and a lower reflector that is 1.585 m high. Helium flows downwards into the lower plenum with an inlet temperature of 259°C at a nominal pressure of 6.4 MPa and a nominal pressure drop of 29.9 kPa (4.33 psi) across the core.

Also shown in Figure 2 is a one-twelfth sector of the block that is bounded on all sides by planes of symmetry. The analysis in the present paper is based on a one-twelfth sector of an entire column.

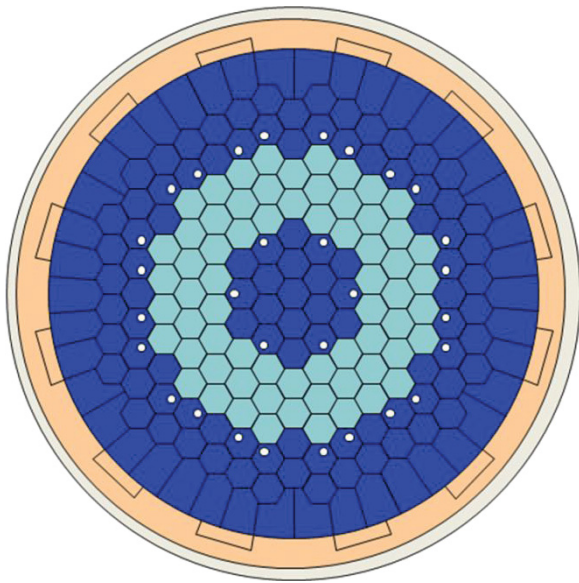


Fig. 1. Cross-sectional view of block VHTR.

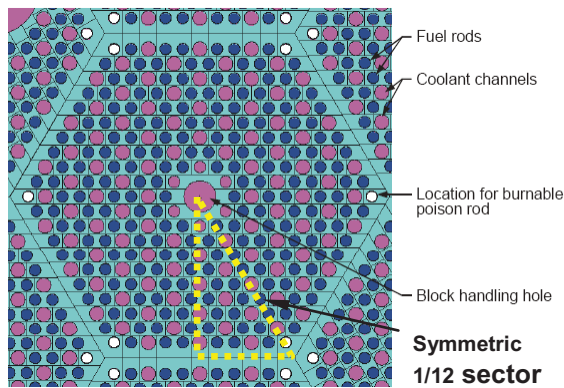


Fig. 2. Plan view of a hexagonal block and one-twelfth symmetric sector.

Between the hexagonal blocks, there are gaps, which are present because of tolerances in machining the blocks and variations in their installation. Also, these gaps will vary with time because of thermal expansion and irradiation. It was decided to perform computational fluid dynamics (CFD) analysis of the flow and heat transfer in the one-twelfth sector of a block that includes the gap to estimate the impact that the flow in the gap, called bypass flow, can have on flow and heat transfer in the core and lower plenum, located below the core.

Other researchers have used a variety of approaches to analyze the flow and heat transfer in a block VHTR. Simple approaches using networks and simplified unit cell methods have been employed, e.g. Takada et al [2] and Nakano et al. [3]. More advanced approaches have also been employed using conjugate flow and heat transfer available in commercial CFD codes. Tak et al. [4] used a symmetric one-twelfth sector of a prismatic block. However, Tak et al. determined inlet flows

from separate 1D code calculations. Recently, Sato et al. [5] employed a similar one-twelfth sector analysis using commercial code FLUENT [6] to investigate the effects of bypass flow for a 600 MW<sub>th</sub> prismatic VHTR, based on a General Atomics Gas-Turbine Modular Helium Reactor (GT-MHR), which originally was used as the reference design for the NGNP [7]. In Ref. [5], the flow rates were determined as part of the solution by using pressure boundary conditions for the inlet and outlet.

## II. CFD MODEL

The approach used in the present investigation is similar to that of Sato et al. [5]. It should be noted that the GT-MHR has 102 fueled columns, as opposed to 66 for the MHTGR, such that the power density for the MHTGR is still about 90% that of the GT-MHR. Also, the inlet temperature for the earlier GT-MHR was 490°C compared to 259°C for the present case.

The CFD model is based on a one-twelfth sector of a prismatic block, as shown in Figure 2, which includes the entire core in the vertical direction with an upper reflector section, 10 fueled blocks and a lower reflector section. Hence, the model is 10.704 m in length. Figure 3 illustrates a cross-section of the CFD mesh, showing fuel and coolant channels. The diameters of the channels are as shown; there is only 1/2 of a small diameter coolant channel in the sector. There are 5 full and 7 half large-diameter coolant channels. It was found in a separate study that the 1/2 coolant channels, with a symmetry boundary, yielded virtually the same flow results as for a full channel [5]. There are 5 half and 15 full fuel channels. Only 1/2 of the gap width is included in the CFD model because of symmetry. All of the side boundaries are set to symmetry conditions. The grid was created using GAMBIT 2.4.6 [6]. A 2-D mesh was extruded in the third direction. The mesh cells are hexahedrons. The mesh has about 7.6 million cells. A finer mesh was also constructed and used to

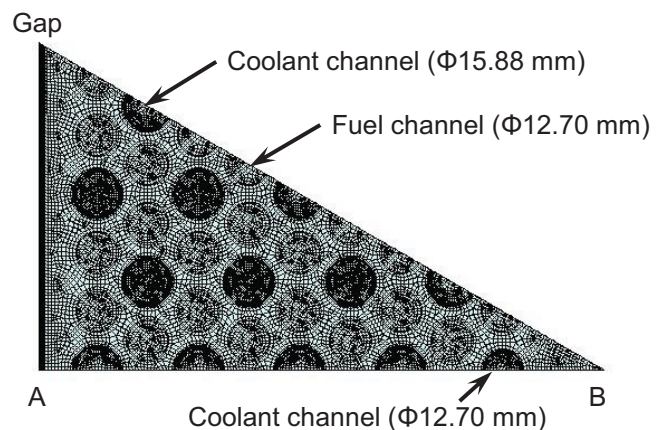


Fig. 3 Plan view of the CFD mesh.

obtain results to check for grid independence; the finer mesh contained 10.9 million cells. The differences in the total mass flow rate, and average coolant channel outlet (absolute) temperatures and maximum fuel temperatures were all less than 0.5% for the 0 mm gap case [5]. The mesh used for all of the present calculations (7.6 million cells) has an overall  $y^+$  of less than 6.

The standard  $k-\epsilon$  turbulence model with the enhanced wall treatment option was employed to account for the turbulence [6]. The enhanced wall treatment is designed to apply all the way to the wall without using wall functions. A calculation was made for a single representative coolant channel using the above turbulence model and the wall shear stress compared to two published friction correlations [6]. It was found that the maximum differences between the computed results and the Zigrang-Sylvester and Blasius correlations were 2.2 % and 0.74 %, respectively, giving confidence that the turbulence model computes the flow accurately. Note that the Reynolds number changes with core depth because the viscosity is a function of temperature.

Calculations were made using the SIMPLE algorithm on a Dell PowerEdge 1950 distributed memory cluster running the OpenSUSE 11.1 operating system. Iterative convergence was obtained by requiring that the default residuals be converged to a tolerance of  $1 \times 10^{-5}$ . This was shown in previous studies to be sufficient, including for fully developed flow in a tube (Poiseuille flow), which has an analytical solution.

Inlet temperature for the several cases was set to 259°C as specified for the MHTGR [1]. The flow was induced by specifying a stagnation pressure inlet and a static pressure outlet. The nominal pressure difference specified is 29.9 kPa for the no gap case. However, the pressure is adjusted in some cases to indicate that the bypass flow is 'stolen' from the coolant channel flow, as will be indicated below.

Helium properties, assumed to be isobaric at 6.4 MPa, are obtained from the National Institute of Standards and Technology website [9]. The graphite properties are based on H-451 graphite [10]. The fuel compact properties are taken from previous thermal hydraulic studies conducted by the INL [7].

For the present calculations, it is assumed that there is no bypass flow horizontally between blocks, there are no cracks in the graphite that would allow flow and the geometry is uniform in the vertical direction. Also, the burnable poison and fuel handling holes are given graphite properties.

Several parametric studies are performed in the present paper. These include:

- a) variation of gap width but maintaining the same overall mass flow rate,

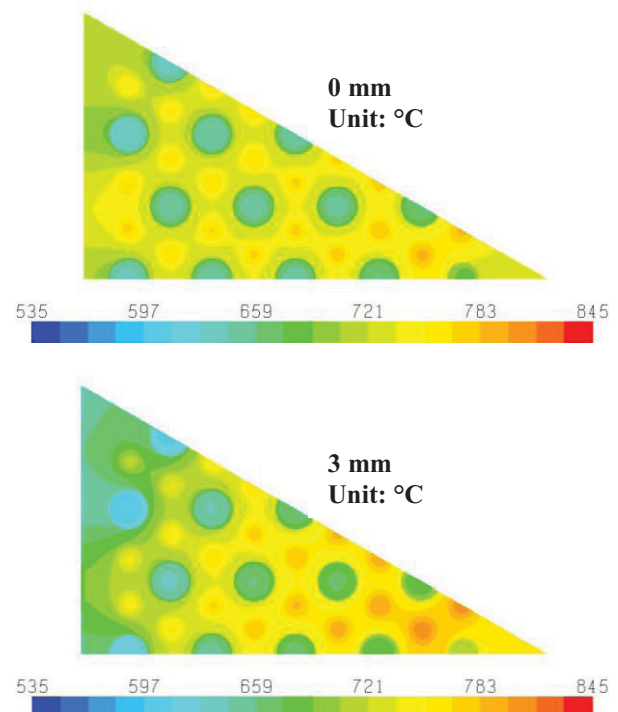
- b) axial variation of heat generation rate at the peak radial factor and
- c) the same as item b but with overall shrinkage from neutron fluence.

### III. RESULTS AND DISCUSSION

#### III.A. Effect of Gap Width for Fixed Mass Flow

The gap width between the prismatic blocks is varied from 0 to 3 to 5 mm. The overall mass flow is kept approximately to a constant rate, which means that the bypass flow is 'stolen' from the coolant channel flow. In the actual application, the presence of bypass flow paths will decrease the overall flow resistance, leading to a higher flow rate and a lower pressure drop than for the case of no bypass flow. The exact variation in pressure head due to the presence of bypass flow will depend on the performance curve of the circulator. The present approach where the pressure difference is decreased to obtain the same flow rate as for the no gap case is probably more severe than will be the actual case. The heat generation rate is set to a constant value for all of the fuel channels at a value of  $25.138 \text{ MW/m}^3$ .

Figure 4 shows temperature contours for the plane that shows the highest fuel temperature, about 0.06 m above the lower edge of the fueled section.



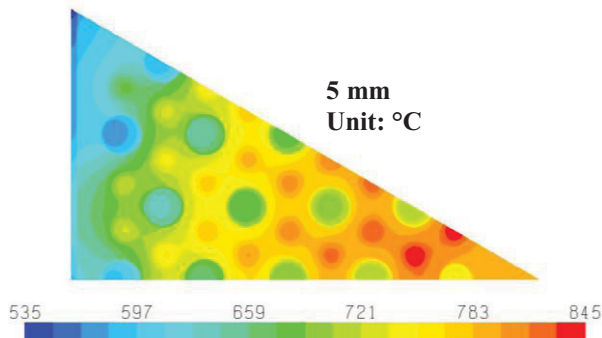


**Fig. 4. Temperature contours for the 0, 3 and 5 mm gap cases for constant mass flow rate.**

As can be seen, the maximum fuel temperature increases significantly as the gap width increases, from 785 to 808 to 841 °C. It can also be seen that the graphite near the gap decreases significantly in temperature, causing a rather larger temperature gradient with increasing gap width. This may have significance for structural integrity because of increased thermal stresses. Figure 5 illustrates the temperature variation from point A to B (see Fig. 3), along the bottom edge of the sector. It is clear that the overall temperature gradient increases as the gap width increases, with the maximum temperature differences in the graphite being 68, 122 and 190 °C for the 0, 3 and 5 mm gap widths, respectively.

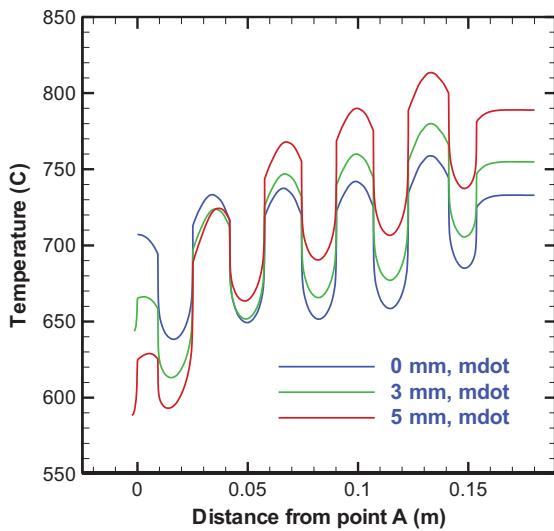


**Fig. 5 Temperature profiles along line A-B for 0, 3 and 5 gap widths.**

Figure 6 illustrates the coolant and gap outlet temperatures and mass flow rates for the three gap width cases for each coolant channel and the gap. Note that the mass flow rates are for the whole channels and the whole gap width. As can be seen, the maximum coolant outlet temperature increases from 685 to 704 to 734 °C for increasing gap width. In addition, the maximum variation in coolant outlet temperature increases dramatically from 36 to 77 to

130 °C for increasing gap width. This has implications on the coolant flow into the lower plenum, because the variation of jet temperatures flowing into the lower plenum is a strong function of gap width. This means that for increased bypass flow, the helium in the lower plenum will require more mixing to even out the temperature.

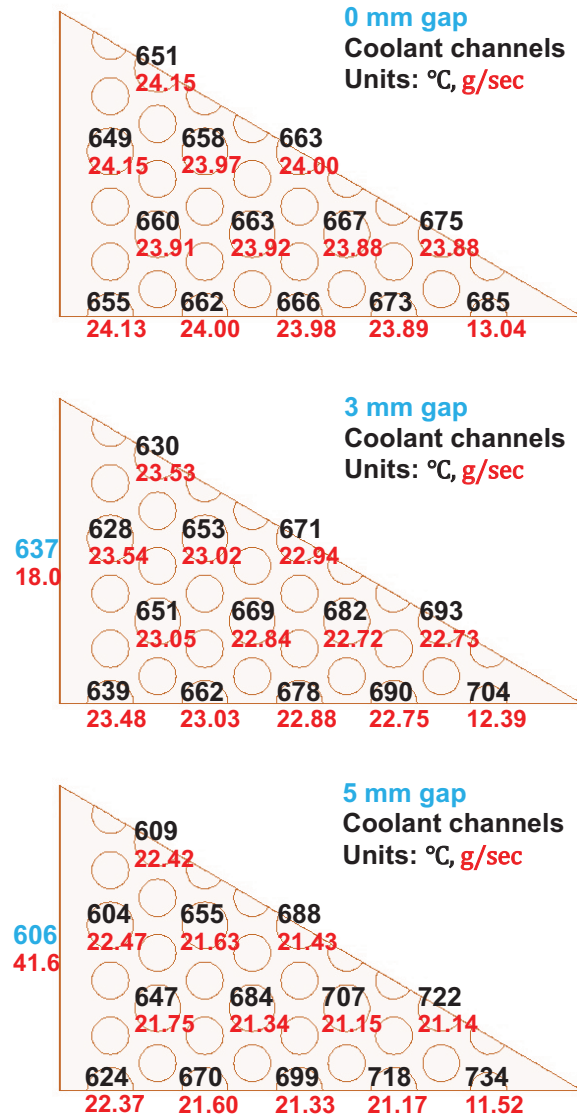


**Fig. 6 Helium temperatures and mass flow rates for 0, 3 and 5 mm gap widths.**

Table 1 shows the input parameters and output results for this study. It can be seen that the pressure difference decreases as the gap width increases to maintain an approximately constant flow rate. The bypass flow percentage, which is based solely on the one-twelfth sector (and includes only the 1/2 channel and 1/2 gap flow rates), is seen to increase significantly with gap width. The maximum fuel and channel temperatures are shown along with the maximum variation in helium temperature. The overall bulk outlet temperatures are about 661 °C.

Gap width mm	0	3	5
Mass flow kg/s	0.210	0.211	0.211
Pressure drop Pa	29900	27782	25024
Gap flow fraction %	0	4.27	9.87
Max fuel temp °C	785	808	841
Gap outlet temp °C	-	637	606
Max channel temp °C	685	704	734
Max helium temp variation °C	36	77	130
Bulk outlet temp °C	662	661	661

Table 1. Inputs and results for the gap width study.

### III.B. Effect of Heat Generation Profile

The previous results employed a constant average heat generation rate in the fueled channels. The actual heat generation profile varies axially and radially in the core. The axial variation typically assumes a cosine profile with the maximum near the center of the core. Additionally, the radial variation can show a maximum of 1.25 [8]. Based on this information, heat generation profiles were generated to represent axial variation at the average and peak radial levels. The heat generation profile is given as

$$\text{—————} \quad (1)$$

where  $q'''$  is the heat generation rate per unit volume,  $A_r$  is the radial factor,  $q_{con}$  is a constant set to the value necessary to obtain the total correct heat generation rate in the core,  $A_p$  is the peak axial factor,  $z$  is the axial coordinate from the top of the prismatic core and  $L$  is the heated core length. The peak and average radial factors are given as 1.25 and 1.0, respectively [8]. The heated core is 7.93 m and the upper reflector has a length of 1.189 m. Figure 7 shows the heat generation profile for the average and peak radial factors with the axial factor set to 1.3 [8].

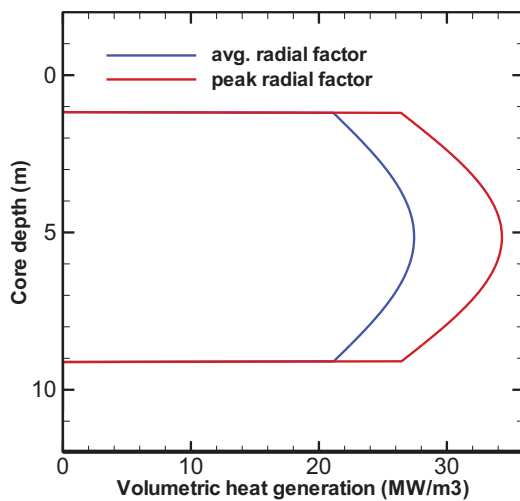


Fig. 7. Volumetric heat generation rates for the average and peak radial factors.

The pressure drop across the core is set to the nominal 29.9 kPa and the gap is set to 3 mm for all cases. Calculations are made for a reference case, which has an average heat generation rate, and for the peak radial profile shown in Figure 7. Results for the average radial factor with axial variation are not presented because they were seen to differ very little from a similar reference calculation for the 600 MW<sub>th</sub> GT-MHR simulations [5].

Figure 8 shows temperature contours for the plane at the hottest fuel temperature, about 0.06 m above the end of the fueled section. Both plots show higher temperatures at the block center and cooler temperatures adjacent to the gap. The overall temperature for the profile for the axial variation at the peak radial factor is significantly higher because of the 25% higher heat generation rate. Note that the contour scale is the same for both plots.

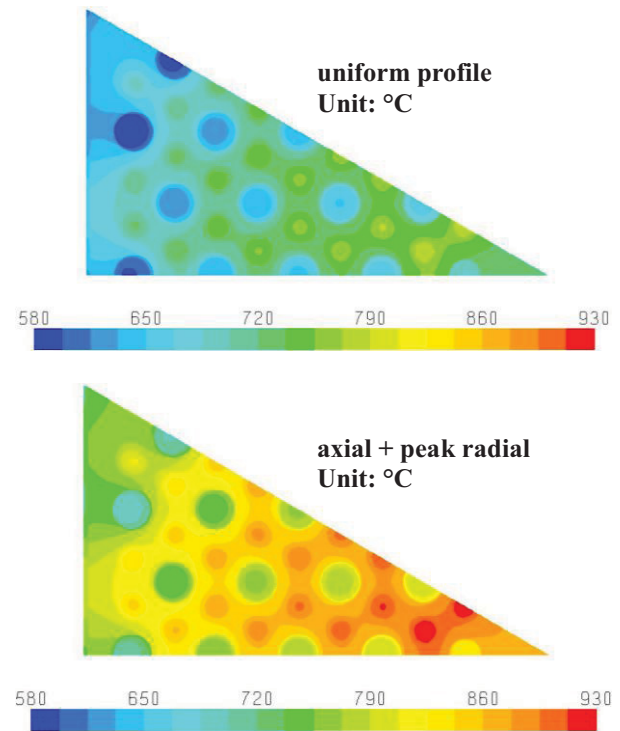


Fig. 8. Temperature contours for the uniform and axial + radial heat generation profiles.

Figure 9 plots the temperature along line A-B for the reference uniform case and the case for axial variation at the peak radial factor. The temperatures for the axial plus peak radial factor are about 150°C higher than for the reference case.

Figure 10 shows bulk outlet temperatures and mass flow rates for the reference uniform case and the case for axial variation at the peak radial factor. Temperature differences between corresponding coolant channels for the two cases vary from between 115 and 137°C. Mass flows for the peak radial case are about 6% lower than for the reference uniform case. Also note that the maximum coolant

temperature is 820°C, 70°C higher than the nominal expected outlet temperature for this reactor design.

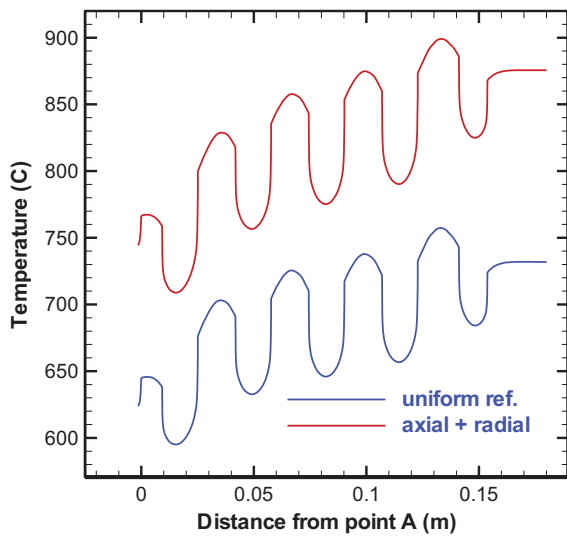


Fig. 9 Temperature profiles along line A-B for the reference uniform and axial + peak radial case.

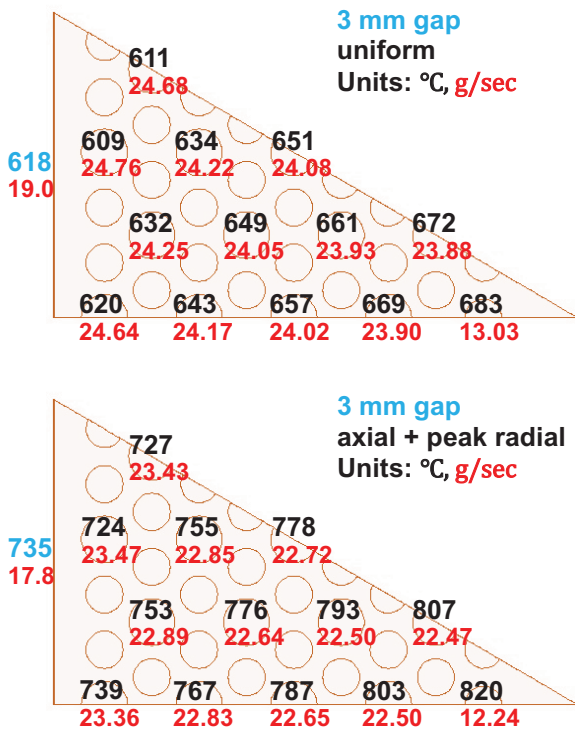


Fig. 10 Helium temperatures and mass flow rates for the reference uniform and axial + peak radial cases.

Table 2 tabulates the input parameters and output results for the reference uniform and the peak radial heat generation rate profile. Note that the mass flow in Table 2 is for the exact one-twelfth sector, whereas the mass flows reported in Figure 10 are for the whole channels and whole gap. Note that the mass flow in the hotter case is lower as expected because the viscosity increases with temperature,

lowering the flow rate. While the gap flow fraction is about the same for the two cases, the maximum fuel and coolant temperatures increase by 141 and 137°C, respectively. The maximum variation in temperature only increases by 11°C for the hotter case. However, the increase in the maximum coolant temperature for the hotter case over the no gap case of Table 1 is 135°C, about the same as the increase for the 5 mm case over the no gap case. This illustrates the potential that increasing gap width for a constant mass flow has to increase the variation in coolant temperature into the lower plenum, which has a direct effect on the level of mixing of the coolant in the lower plenum, one of the main concerns for the lower plenum. That is, it is much better that the coolant temperature be close to uniform to avoid problems in the downstream hardware, whether it be a turbine or an intermediate heat exchanger (IHX). The overall bulk outlet temperature for the peak radial case is 124 °C higher than for the reference case.

Heat profile	uniform	axial+radial
Pressure drop Pa	29900	29900
Mass flow kg/s	0.222	0.209
Gap flow fraction %	4.28	4.25
Max fuel temp °C	786	927
Gap outlet temp °C	618	735
Max channel temp °C	683	820
Max helium temp variation °C	74	85
Bulk outlet temp °C	641	765

Table 2. Inputs and results for variation of the heat generation rate.

### III.C. Effect of irradiation shrinkage

This study investigates the effects of irradiation-induced change in the geometry of the graphite block region to flow and temperature distributions in the reactor core. The one-twelfth sector column reference grid is shrunk by 1.23% in the radial direction and by 2.35% in axial direction uniformly. These geometric changes are maximum dimensional changes experienced by H451 graphite from irradiation [9]. The shrinkage in the radial direction increases the gap width and shrinks the diameters of the coolant channels. Uniform dimensional change in the axial direction shrinks the length of the hexagonal block. As a result, the gap width increases from the assumed nominal 1 mm to 5.5 mm, and the total length of the one-twelfth sector shrinks from 10.704 m to 10.45 m. Calculations are made for the above case and compared to a reference case where no shrinkage occurs; the reference case is also assumed to have a 5.5 mm gap width. The differential pressure is predetermined parametrically to obtain the same total flow rate as the 0 mm gap-

width case in Section 4.1, which is 0.21 kg/sec. Nonuniform heat generation with axial variation at the peak radial factor ( $A_p = 1.3$  and  $A_r = 1.25$ , respectively) is applied to both the shrinkage and the reference no-shrinkage cases in order to accentuate the impact of geometrical change on the temperature distribution in the fuel column.

Figure 11 shows contour plots of temperature at the hottest planes for the reference case of no-shrinkage and shrinkage cases. The hottest plane for the no-shrinkage case is located at 0.099 m above the end of the fueled section, but at 0.06 m above the fueled section for the shrinkage case. The no-shrinkage case shows higher temperatures than the shrinkage case. The main reason for this is that in order to obtain similar mass flow rates, the pressure drop for the shrinkage case must be higher, increasing the Reynolds number and, hence, the heat transfer, thus, lowering the temperatures for the shrinkage case. The temperatures are also lower in the region adjacent to the gap.

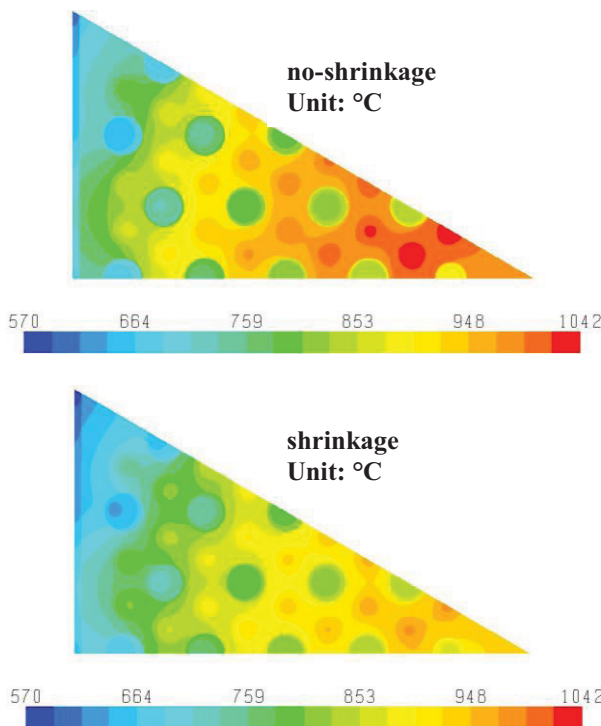


Fig. 11. Temperature contours for the reference no-shrinkage and shrinkage cases.

Figure 12 plots the temperature along line A-B for the two cases. The temperature difference is about 60°C in the graphite, but within 15°C in the coolant channels. Figure 13 illustrates the bulk temperatures and mass flow rates for the two cases at the outlet to the lower plenum. The temperatures are only slightly lower for the shrinkage case while the mass flow rates are slightly higher for the shrinkage case.

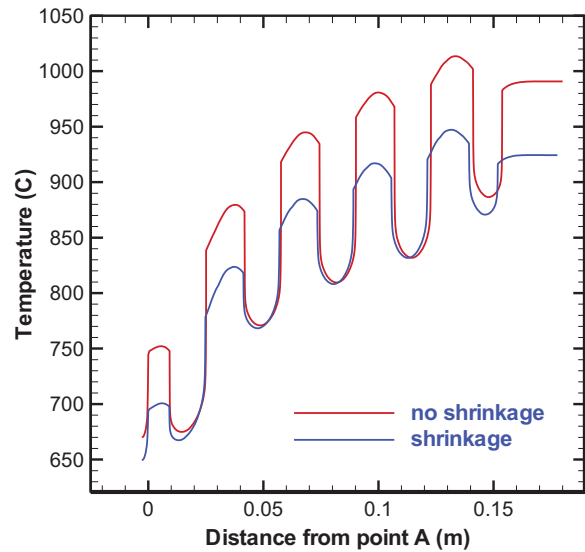


Fig. 12 Temperature profiles along line A-B for the no-shrinkage and shrinkage cases.

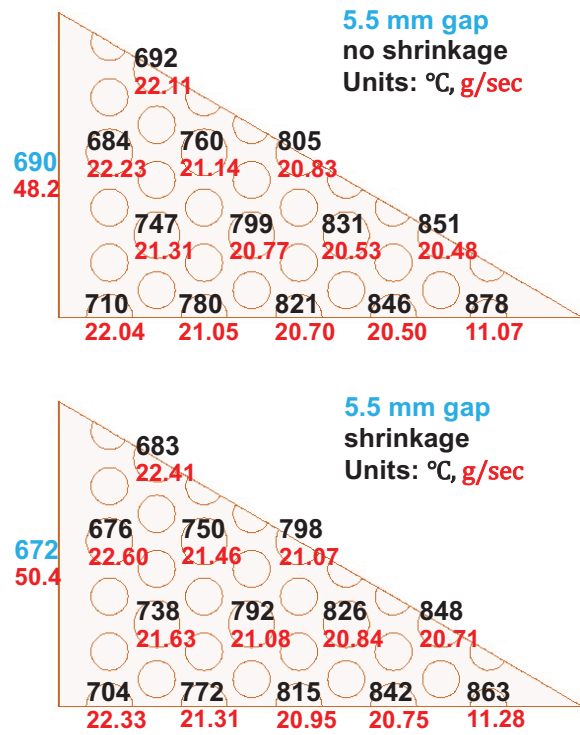


Fig. 13 Helium temperatures and mass flow rates for the no shrinkage and shrinkage cases.

Table 3 provides a summary of the inputs and results for the no-shrinkage and shrinkage cases. The pressure difference is about 5.6% higher for the shrinkage case to obtain approximately the same total mass flow rate of about 0.21 kg/sec. The gap flow fraction is relatively high for both cases at 11.5 and 11.8% for the no-shrinkage and shrinkage cases, respectively. The maximum fuel temperatures are the highest seen so far at 1041 and 976 °C for the two cases. Also, the maximum temperature variation

in coolant temperature is the highest seen at about 190°C for the two cases. Finally, the overall bulk outlet temperatures is close to 760°C for the two cases, about the same as for the previous case of axial + peak radial heat generation profile in Table 2.

Heat profile	no-shrinkage	shrinkage
Pressure drop Pa	26345	27810
Mass flow kg/s	0.209	0.213
Gap flow fraction %	11.50	11.81
Max fuel temp °C	1041	976
Gap outlet temp °C	690	672
Max channel temp °C	878	863
Max helium temp variation °C	194	191
Bulk outlet temp °C	765	756

Table 3. Inputs and results for no-shrinkage and shrinkage cases.

#### IV. SUMMARY AND CONCLUSIONS

The 3-D conjugate heat transfer and fluid flow calculations for a one-twelfth sector of a fuel column in a reference 350 MW<sub>th</sub> prismatic VHTR are conducted using commercial CFD code FLUENT in order to investigate the influence of several factors related to bypass flow on flow and temperature distribution in the reactor core. Parametric studies varying the factors including gap width for a constant mass flow rate, variable heat generation profile, and geometry changes resulting from irradiation shrinkage in the prismatic block, are conducted to understand the effects of core bypass flow. The study revealed that flow and temperature distributions in the prismatic fuel assembly are strongly coupled and therefore detailed 3-D thermal hydraulic analyses using CFD, which can take local physics into account, is an effective method for evaluating the coolant bypass phenomena. In particular, the flow rates of coolant in the channels and in the interstitial gaps are a function of the solution and are not known a priori. The following conclusions are drawn from these studies:

- Bypass flow in the gap provides a significant cooling effect on the prismatic block.
- Bypass flow establishes a large lateral temperature gradient in the block.
- The maximum fuel temperature and maximum coolant channel outlet temperature are significantly increased by an increase of gap width in the bypass flow if the gap flow is 'robbed' from the coolant channel flow. This conclusion indicates that the bypass flow has a significant effect on hot spots in the core and on the variation in temperature of jets flowing from the core into the lower plenum.

- An increase in heat generation rate increases the temperature of the helium in the channels, gap, graphite, and fuel, but it decreases the coolant flow rates in the channels and gap.
- Irradiation-caused shrinkage of the prismatic block produces a slight increase in gap flow ratio and a decrease in maximum fuel temperature.

#### ACKNOWLEDGEMENT

Work supported by the U.S. Department of Energy, Office of Nuclear Energy, under DOE Idaho Operations Office Contract DE-AC07-05ID14517.

#### REFERENCES

- [1] GA Technologies, Inc., Preliminary Safety Information Document for the Standard MHTGR, document HTGR-86-024, rev. 13, 1992.
- [2] E. Takada, S. Nakagawa, N. Fujimoto, D. Tochio, Core Thermal-Hydraulic Design, Nuclear Engineering and Design, 233, 37-43, 2004.
- [3] M. Nakano, N. Tuji, N., Y. Tazawa, Conceptual Reactor Design Study of Very High Temperature Reactor (VHTR) with Prismatic-Type Core, Journal of Power and Energy Systems, 2(2), 768-774, 2008.
- [4] N. Tak, M. Kim, W. Lee, Numerical investigation of a heat transfer within the prismatic fuel assembly of a very high temperature reactor, Annals of Nuclear Energy, 35, 1892-1899, 2008.
- [5] H. Sato, R. W. Johnson, R. R. and Schultz, Computational Fluid Dynamic Analysis of Core By-pass Flow Phenomena in a Prismatic VHTR, to appear in *Annals of Nuclear Energy*.
- [6] FLUENT Inc., FLUENT, version 6.3.26, Lebanon, NH, USA, 2006.
- [7] P. MacDonald, J. Sterbentz, R. Sant, P. Bayless, R. Schultz, H. Gougar, R. Moore, A. Ougouag, W. Terry, NNGP Preliminary Point Design Results of the Initial Neutronics and Thermal-Hydraulic Assessments, INEEL/EXT-03-00870, 2003.
- [8] R. W. Johnson and R. R., Schultz, Bounding Estimate for the 'Hot' Channel Coolant Temperature and Preliminary Calculation of Mixing in the Lower Plenum for the NNGP Point Design Using CFD, INEEL/EXT-04-02570, Rev. 1, 2004.
- [9] <http://webbook.nist.gov/chemistry/fluid/>
- [10] General Atomics, Safety Analysis Report use of H451 Graphite in Fort St. Vrain Fuel Elements, GLP-5588, 1977.